

## Article

# A Preliminary Study for Tunable Optical Assessment of Exhaled Breath Ammonia Based on Ultrathin Tetrakis(4-sulfophenyl)porphine Nanoassembled Films

Sergiy Korposh <sup>1</sup>  and Seung-Woo Lee <sup>2,\*</sup> 

<sup>1</sup> Department of Electrical and Electronic Engineering, University of Nottingham, Nottingham NG7 2RD, UK; s.korposh@nottingham.ac.uk

<sup>2</sup> Graduate School of Environmental Engineering, The University of Kitakyushu, 1-1 Hibikino, Kitakyushu 808-0135, Japan

\* Correspondence: leesw@kitakyu-u.ac.jp; Tel.: +81-93-695-3293

**Abstract:** The detection of chemical substances excreted from the human body offers an attractive approach for non-invasive, early diagnostics of certain diseases. In this preliminary study, we proposed a susceptible optical sensor capable of quantitatively detecting ammonia from exhaled breath. The proposed sensor consists of nanoassembled ultrathin films composed of tetrakis(4-sulfophenyl)porphine (TSPP) and poly(diallyldimethylammonium chloride) (PDDA) deposited on quartz substrates using a layer-by-layer method. Measurement principles are based on the ammonia-induced absorbance changes at 489 (Soret band) and 702 nm (Q band), associated with the deprotonation of the J-aggregated TSPPs inside the film. Before exposure to breath, the PDDA/TSPP thin film was calibrated using known concentrations of ammonia gases with a projected detection limit of  $102 \pm 12$  parts per billion (ppb). Calibrated sensor films were then exposed to human breath and urine samples to determine the ammonia concentration. Concentrations of exhaled ammonia are influenced significantly by the consumption of food or the amount of urea. Sensor response and maximum sensitivity, obtained from the absorbance changes induced by ammonia, were achieved by initial sensor exposure to HCl vapor. Previously reported procedures for the *Helicobacter pylori* (HELIC Ammonia Breath) test based on urea reaction with urease were reproduced using the proposed sensor. The observed behavior corresponded very well with the kinetics of the interactions between urea and urease, i.e., ammonia reached a maximum concentration approximately 5 min after the start of the reaction. A large-scale study involving 41 healthy volunteers in their 20s to 60s was successfully conducted to test the capabilities of the sensor to determine the concentration of exhaled ammonia. The concentration of ammonia for the healthy volunteers ranged between 0.3 and 1.5 ppm, with a mean value of ca. 520 ppb in the morning (before eating) and ca. 420 ppb in the afternoon (immediately after eating). These real-test mean values are meaningful when considered against the projected LOD.

**Keywords:** breath ammonia; urine; optical sensor; porphyrin; layer-by-layer; nanoassembled film



**Citation:** Korposh, S.; Lee, S.-W. A Preliminary Study for Tunable Optical Assessment of Exhaled Breath Ammonia Based on Ultrathin Tetrakis(4-sulfophenyl)porphine Nanoassembled Films. *Chemosensors* **2021**, *9*, 269. <https://doi.org/10.3390/chemosensors9090269>

Academic Editor: Antonio Fernandez

Received: 17 July 2021

Accepted: 14 September 2021

Published: 18 September 2021

**Publisher's Note:** MDPI stays neutral with regard to jurisdictional claims in published maps and institutional affiliations.



**Copyright:** © 2021 by the authors. Licensee MDPI, Basel, Switzerland. This article is an open access article distributed under the terms and conditions of the Creative Commons Attribution (CC BY) license (<https://creativecommons.org/licenses/by/4.0/>).

## 1. Introduction

Ammonia (NH<sub>3</sub>; CAS No. 7664-41-7) is a major metabolite involved in many physiological processes and a potential biomarker for several diseases [1–5]. A normal, physiological level of ammonia in the blood is between 11 and 50 μM and could be as high as 1 mM during certain pathological conditions [1]. Testing ammonia by using blood samples is fraught with a number of difficulties, such as sample collection, handling, and preparation for analysis [1,6,7]. Although numerous studies have focused on finding a correlation between ammonia in the breath and ammonia in the blood, there is still ambiguity as to whether a correlation actually exists [1,8]. A few studies have found a correlation between the measurements of ammonia in the breath and blood despite limited sensitivity [9–11],

whereas other studies found no clear correlation between concentrations of ammonia in the blood and breath [11,12]. Nevertheless, there is general agreement that exhaled ammonia can be used as a marker of clinically relevant information [1,8,13].

Under normal physiological conditions, ammonia can be expelled from slightly alkaline blood or serum, and it can diffuse through the skin and into the breath. Dysfunctions in the kidney and liver, which convert ammonia to urea, can result in an increase in the concentration of ammonia in breath and urine. The concentration of exhaled ammonia, which was allowed to bypass the upper airway, was found to be in good agreement with concentrations in the blood [9]. Consequently, ammonia in the breath or urine can be used for the early diagnosis of liver or stomach disease [14]. The application of suitable technologies, followed by clinical evidence and trials, has the potential to lead to a broad range of screening, monitoring, and diagnostic solutions for the conditions discussed [1]. The development of portable, cheap, and reliable sensors to measure ammonia concentration with 50–2000 parts per billion (ppb) sensitivity and a fast response time is highly desirable [15]. Conventional methods for ammonia measurement are mainly based on gas-chromatography–mass spectrometry [16,17], which, despite high selectivity and sensitivity, is expensive, requires a well-trained operator, and is time-consuming. One of the major challenges for breath sensor development and deployment is the requirement that measurements must be performed at high humidity (>90%) and high CO<sub>2</sub> levels [8]. The development of cheap, small, sensitive, and reliable sensors that can efficiently operate at different relative humidity levels could create a point-of-care medical system that can be used in daily life.

Optical sensors offer several advantages over their counterparts, such as immunity to electromagnetic interference, biocompatibility, and high sensitivity. In the past decades, various studies have developed approaches to optical fiber-based ammonia sensing by using sensitive coatings. We have recently developed several types of optical ammonia sensors with high sensitivity and selectivity that are capable of detecting ammonia in both liquid medium [18] and gas phase [19,20]. In terms of ammonia selectivity, an optical-based sensor composed of a thin poly(diallyldimethylammonium chloride) (PDDA) and tetrakis-(4-sulfophenyl)porphine (TSPP) film was tested to understand its response to potential interferents, such as volatile organic compounds or volatile organic amines [21]. No clear changes were observed in the UV–vis spectra for organic volatiles such as chloroform, acetone, methanol, ethanol, acetic acid, benzene, and toluene; by contrast, significant optical changes in the two Soret bands and the Q band were obtained when the film was exposed to organic amine vapors, such as trimethylamine, triethylamine, and pyridine. Among organic amine vapors, the only pyridine is found in human breath with concentrations between 0.12–100 ppb and a median value of 11 ppb [22,23], which is much lower than the limit of detection (LOD) of the sensor [20,21]. Fortunately, the fabricated film shows satisfactory cross-sensitivity toward both ammonia and volatile organic amines; in particular, its sensitivity to ammonia is much better than to the volatile organic compounds including amines [20,21].

This study describes the development of an optical sensor to detect ammonia in the breath and urine samples from human subjects, which is based on the layer-by-layer (LbL) nanoassembly of PDDA and TSPP on a quartz plate previously reported in our work [21]. Ammonia-induced absorbance changes were measured as sensor responses by exposing the ultrathin PDDA/TSPP film to the samples of exhaled breath and urine vapor for 10 s and 5 min, respectively. The sensor performance was significantly improved as compared to our previous work [21] by exposing the prepared PDDA/TSPP film to HCl gas, which enables us to fully protonate TSPP and allows the detection of very small concentrations of ammonia (<200 ppb). Moreover, after sample measurements, sensor performance was fully recovered using a vapor produced from a 0.1 M HCl solution. The effects of food and interference of relative humidity were carefully monitored and evaluated in this study. The results obtained from a large-scale study of 41 healthy volunteers demonstrate that

the current sensor has the potential to be deployed in medical applications for the early diagnosis of kidney, stomach, or liver disease.

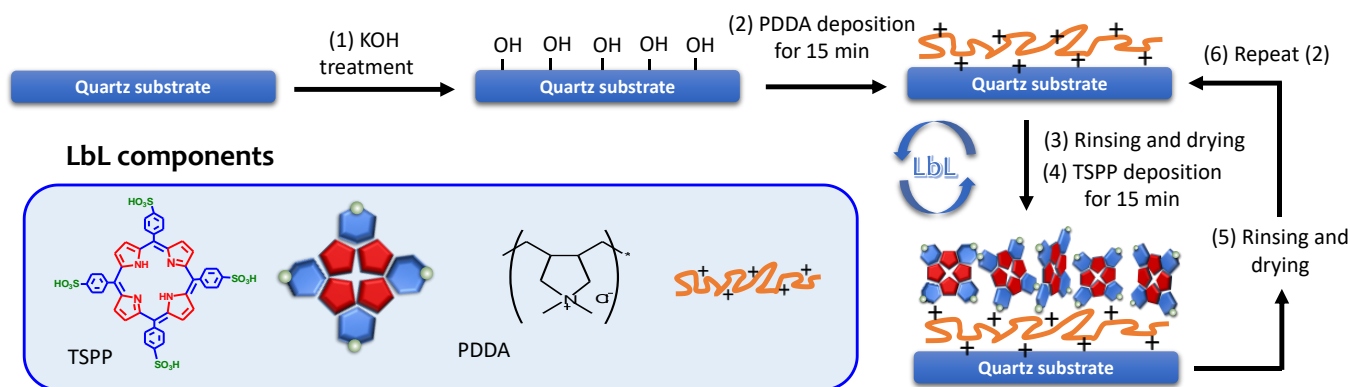
## 2. Materials and Methods

### 2.1. Materials

TSPP and sodium hydroxide (NaOH) were purchased from Tokyo Chemical Industry Co., Ltd. (Tokyo, Japan). PDDA (Mw: 200,000–350,000, 20 wt% in H<sub>2</sub>O) and ammonium hydroxide (28 wt%) were purchased from Sigma-Aldrich (St. Louis, MO, USA). Urea was purchased from Kanto Chemical Co., Ltd. (Osaka, Japan). All chemicals were reagents of analytical grade and used without further purification. Deionized pure water (18.2 MΩ·cm) was produced using a Direct-QTM instrument (EMD Millipore, Billerica, MA, USA), which performed reverse osmosis, ion exchange, and filtration.

### 2.2. Film Preparation

Details of the electrostatic LbL adsorption method employed to deposit the porphyrin thin films onto the quartz substrate are described as follows. Briefly, as shown in Scheme 1, prior to film deposition the quartz substrate was rinsed in ethanol and deionized water several times and treated with 1 wt% of ethanolic KOH (ethanol/water = 3:2, *v/v*) for 20 min to activate the surface with OH groups. After that, the quartz substrate was rinsed with deionized water and dried with nitrogen gas. The film deposition was carried out using PDDA (5 mg mL<sup>-1</sup> in water for 15 min) and TSPP (1 mM in water for 15 min), where one cycle is a combined PDDA/TSPP bilayer, by introducing the quartz substrate into the deposition glass vial of 10 mL with intermediate processes of rinsing in water and drying by flushing with nitrogen gas between layer applications. Every deposition was conducted immediately after drying the quartz substrate with nitrogen gas. Hereinafter, a ten cycle-deposited film is denoted as (PDDA/TSPP)<sub>10</sub>.



**Scheme 1.** Schematic of the electrostatic LbL deposition of PDDA and TSPP for preparing a sensing film.

### 2.3. Calibration of the Sensor Response to Ammonia

Before quantifying the ammonia concentration in breath and urine, the sensitivity of PDDA/TSPP film was first measured by exposing it to vapors of aqueous ammonia solutions of varying concentrations (from 0 to 1000 ppm in solution). The PDDA/TSPP film was placed into a 50 mL glass vial containing 2 mL of different concentrations of NH<sub>4</sub>OH. The concentration of ammonia in the gas phase was measured using ammonia detection gas tubes (Gas Tech, Inc., Ayase, Japan). Ammonia concentrations were determined by changes in the color of the reactive material in the gas tube. The LOD for ammonia in the gas tube is estimated to be approximately 0.2 ppm. A relationship between the concentrations of NH<sub>4</sub>OH in the solution and the corresponding gas concentrations in the headspace is plotted in Figure 1 (Table S1).

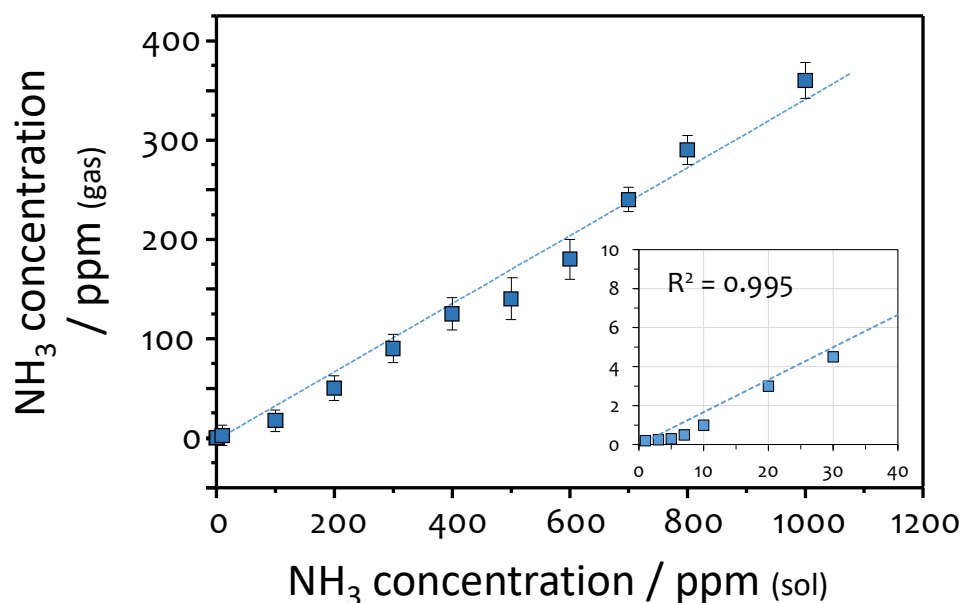


**Figure 1.** Dependence of the ammonia concentrations in the gas phase on the ammonia concentrations in the solution. The inset shows a narrower concentration range below 30 ppm (sol).

#### 2.4. Measurements of Ammonia in Breath and Urine

Figure 2 shows the schematic illustration of the measurement setup used for ammonia detection in breath and urine samples using the PDDA/TSPP film deposited onto the quartz substrate. At first, the PDDA/TSPP film was placed in a 50 mL glass vial, and the breath sample was collected by directly blowing for 10 s into the vial, as shown in Figure 2a. Afterward, the PDDA/TSPP film absorption spectrum was measured, as shown in Figure 2b. For urine headspace ammonia measurements, the PDDA/TSPP film was placed in a 50 mL glass vial containing 2 mL of urine for 5 min. Careful attention was taken to ensure that the sensor film was not in physical contact with the urine sample (Figure 2a).

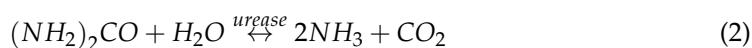
The effects of food consumption on the exhaled ammonia concentration were analyzed using samples collected before food consumption (early morning) and immediately after lunchtime meal. After completing the breath and urine spectra measurements, the PDDA/TSPP film was placed in a 50 mL glass vial containing 2 mL of a 0.1 M HCl solution for 5 min to return the absorption spectra to their initial values (Figure 2a).

A spectrometer (S1024DW, Ocean Optics, FL, USA) and a deuterium-halogen light source (DH-2000-BAL, Ocean Optics, FL, USA) were used to monitor the film assembly and ammonia gas sensing (Figure 2b). Spectra Suite<sup>®</sup> Spectrometer Operating Software (Ocean Optics, FL, USA) was used for the analysis. Absorbance,  $A(\lambda)$ , was determined by taking the logarithm of the ratio of the transmission spectrum of the quartz substrate with a (PDDA/TSPP)<sub>10</sub> film (i.e.,  $T(\lambda)$ ) and the transmission spectrum measured prior to film deposition (i.e.,  $T_0(\lambda)$ ).

$$A(\lambda) = -\log \frac{T(\lambda)}{T_0(\lambda)} \quad (1)$$

#### 2.5. Urea Test

Previously reported procedures [24,25] for the *Helicobacter pylori* (HELIC Ammonia Breath) test were repeated in this study. The subject was asked to consume 5 mL of a 1 M aqueous urea solution, followed by rinsing the mouth cavity with distilled water. According to Equation (2), ammonia and carbon dioxide can be generated via the hydroxylation of urea by urease present in the stomach.



Exhaled ammonia was measured immediately (0 min) and at 5, 10, 15, and 20 min after urea ingestion using the procedures described in Section 2.4.

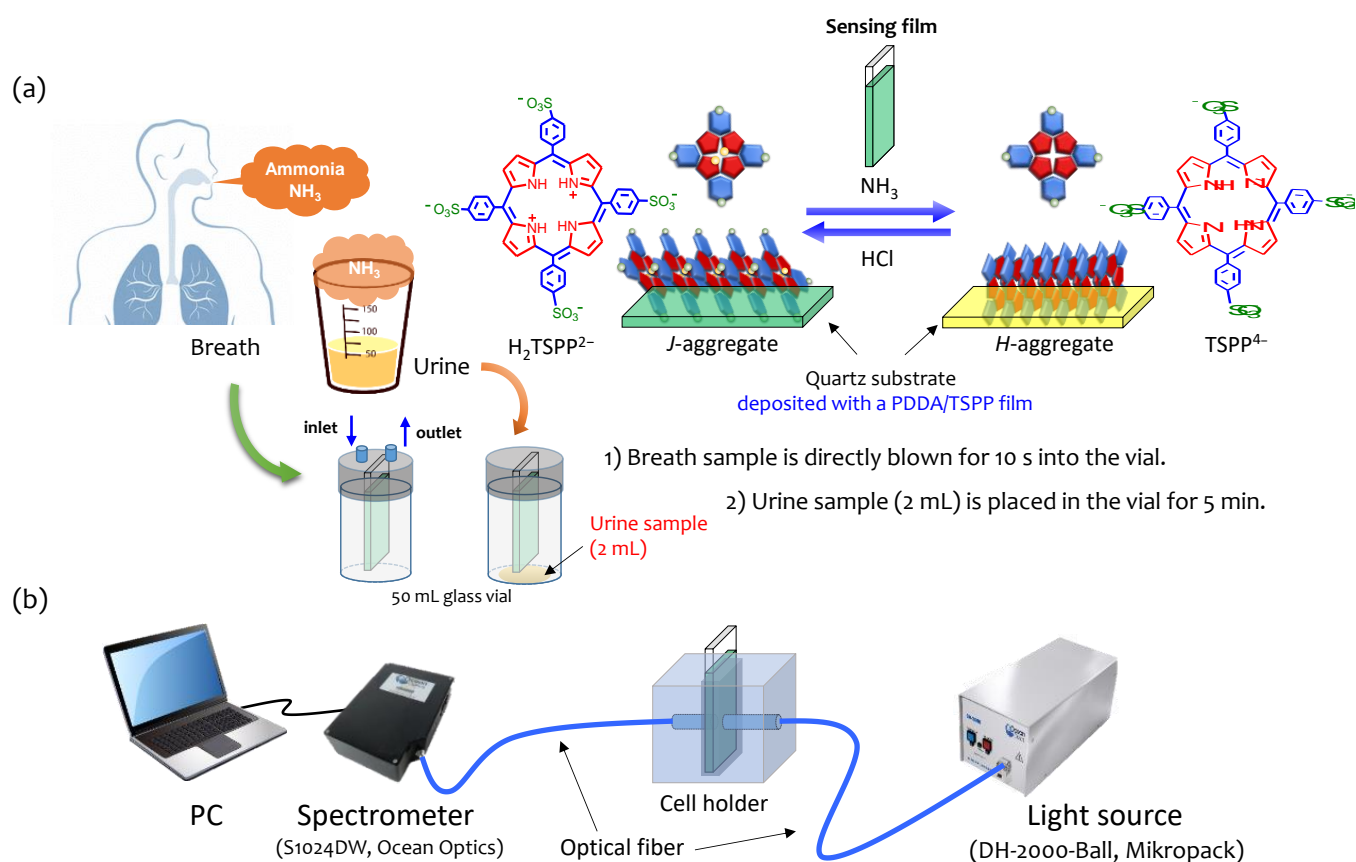


**Figure 2.** (a) Schematic of the sensing principle of ammonia included in breath and urine samples using a PDDA/TSPP LbL film deposited onto a quartz substrate via sensor recovery by HCl vapor treatment. (b) Measurement setup for UV-vis spectra acquisition of the sensor film after exposure to ammonia gas or HCl vapor.

### 2.6. A Large-Scale Study

To test the developed sensor system, a large study was conducted using 41 healthy male and female volunteers in their 20 s to 60 s. Ethical approval was obtained for all breath and urine headspace measurements, and informed consent was obtained from each subject. The procedure for ammonia measurements was identical to that described in Section 2.4.

## 3. Results and Discussion

### 3.1. PDDA/TSPP Film Deposition and Sensitivity Improvement

Figure 3a shows the evolution of absorption spectra during the PDDA/TSPP film deposition onto the glass substrate by using the LbL method. The absorption spectra of the PDDA/TSPP film have a characteristic double peak in the Soret band at 429 and 489 nm and a pronounced Q band peak at 702 nm (Figure 3a). These spectral characteristics suggest that the TSPP molecules in the film preferentially form a J-aggregate. Absorbance by the two Soret bands and the Q band increased linearly (ca. 0.03 a.u./layer) with an increasing number of deposition cycles (inset in Figure 3a), indicating that the LbL method allows a regular film deposition with the linear change at 429 nm.

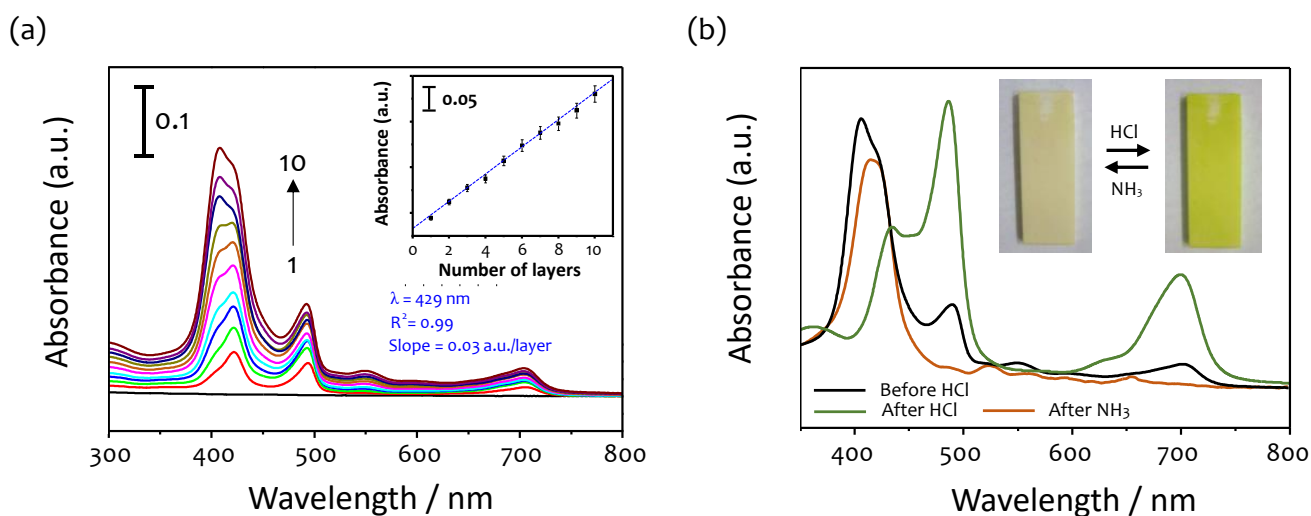


**Figure 3.** (a) Evolution of the UV–vis spectra during the deposition of the PDDA/TSPP film onto the quartz substrate. (b) UV–vis spectral changes of the 10-cycle PDDA/TSPP film: the black line represents the absorption spectrum of the as-prepared film, and the green and brown lines represent the absorption spectra after exposure to the HCl (0.1 M) vapor and ammonia (0.1 wt%) gas, respectively. The inset in Figure 3b shows a photo image of the 10-cycle PDDA/TSPP film deposited on a white acrylic plate, depicting the color change after exposure to HCl vapor or ammonia gas.

To increase the population of *J*-aggregated TSPPs in the film, the as-prepared PDDA/TSPP film was exposed to HCl vapor (produced by an aqueous solution of 0.1 M HCl) before exposure to ammonia. As observed in Figure 3b, the absorbance of the Soret band at 489 nm and the Q band at 702 nm were significantly enhanced when the film was treated with HCl, thus suggesting that exposure to HCl gas increased the relative population of *J*-aggregated TSPPs in the film. This is also confirmed from the photo image in the inset of Figure 3b, showing that a similarly prepared thin film on a white acrylic plate exhibits a bright green color after exposure to HCl vapor. Interestingly, this green color related to the enhancement of *J*-aggregated TSPPs in the film immediately changed to light yellow when the film was exposed to ammonia vapor (produced by an aqueous solution of 0.1 wt% ammonia) for 60 s. This induces the disappearance of the Soret band at 489 nm and the Q band at 702 nm. As was reported previously [20,21], ammonia detection using a thin film composed of TSPP is based on the deprotonation of the pyrrole ring during the exposure to ammonia gas. Increasing the amount of TSPP in protonated form improves the sensitivity of the sensor film to ammonia gas. It should also be noted that water vapor protonates TSPP similar to HCl, and the oversaturation of *J*-aggregated TSPPs in the film via HCl protonation makes it possible to minimize its response to exposure to water vapor.

### 3.2. Response to Ammonia

Figure S1a shows the absorption spectra of the PDDA/TSPP film measured after exposure to ammonia vapors produced by various concentrations of ammonia solutions. Exposure to ammonia induces a drastic change in the second Soret band and the Q band located at 489 and 702 nm, respectively. This observation indicates that ammonia disturbs the *J*-aggregation of TSPP, which is in good agreement with previously reported behavior [18,21]. To estimate the ammonia concentration in the gas phase produced by ammonia solutions at different concentrations, gas tubes were used, as described previously. The ammonia concentration in the gas phase proportionally increased with the increase in the ammonia concentration in the solution (Figure 1 and Table S1). In Figure 4a, the PDDA/TSPP film readily responds to ammonia in the gas phase with a concentration of less than approximately 0.3 ppm. The corresponding change in absorbance at the second Soret band (489 nm) is approximately 0.02, thus suggesting that it is possible to successfully measure samples with concentrations significantly lower than 0.3 ppm ammonia gas. The

mean ammonia concentration of exhaled ammonia collected from the participants of the previous study was reported to be approximately 0.9 ppm with a maximum value of 3 ppm [1]. The PDDA/TSPP film is sensitive to ammonia concentrations as low as 0.3 ppm. Therefore, exhaled ammonia can be measured reliably.

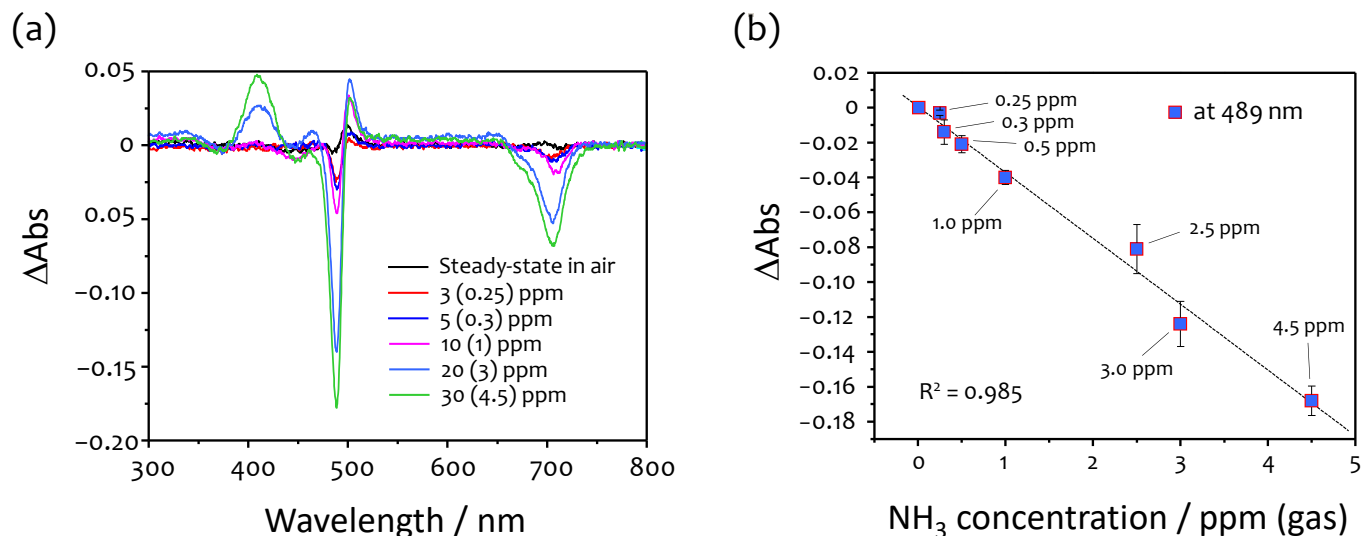


**Figure 4.** (a) Difference absorption spectra of the PDDA/TSPP film measured after exposure to ammonia gases with varying concentrations and (b) the dependence of the absorption value at 489 nm on the concentrations of ammonia in the gas phase.

The response of the PDDA/TSPP film is linear and sensitive to a level of  $0.038 \pm 0.002$  a.u./ppm (Figure 4b). Ammonia concentration measurements were replicated three times at each concentration, and error bars represent the standard deviation of these three measurements. By taking into account the standard deviation (0.001) of blank measurements (Figure S2), the projected LOD for the PDDA/TSPP film when measuring ammonia concentration was calculated to be  $102 \pm 12$  ppb by using Equation (3) [26].

$$\text{LOD} = 3.3 \frac{\sigma}{m} \quad (3)$$

where  $\sigma$  is the standard deviation of the blank measurements (the PDDA/TSPP film absorbance value at 489 nm after HCl vapor treatment and before exposure to ammonia gas), and  $m$  is the slope of the calibration curve. Sensor regeneration is accomplished simply by exposing the PDDA/TSPP film to an aqueous solution of 0.1 M HCl for 15 min. It should be noted that ammonia gas concentrations ( $<1$  ppm) measured using the gas tube tend to deviate from the calibration curve (Figure 1). This small deviation from linearity may be related to the sensitivity of the gas tube that has an LOD of approximately 0.2 ppm for ammonia. On the other hand, as can be seen from the results in Figure 4, the ammonia gas concentrations below 5 ppm, which were estimated from the calibration curve in Figure 1, reveal good linearity for the corresponding absorbance changes at 489 nm, suggesting that low ammonia gas concentrations below 1 ppm linearly correlate with those generated from the corresponding aqueous solutions. Namely, this observation indicates that ammonia gas concentrations larger than the projected LOD can potentially be measured reliably.

### 3.3. Humidified Breath Ammonia Detection and Selectivity

As mentioned previously, exposure to water vapor has a similar effect as that of HCl, and absorbance values at both the second Soret band (489 nm) and the Q band (702 nm) slightly increased after the first HCl treatment of the film (red line in Figure 5a). However, the protonation of TSPP caused by water vapor is very small compared to that due to the exposure to HCl vapor, which may be ignorable. In other words, the water vapor protonates TSPP molecules in the film but the protonated form cannot reach saturation

levels. Interestingly, the TSPP protonation could be saturated via additional HCl treatment for 15 min (green line in Figure 5a). After the secondary HCl treatment of the film, water has minimal effect on the absorption spectra of the TSPP (blue line in Figure 5a) and there were no significant changes, even with continuous exposure to water vapor for 15 min each (Figure S1b). This allows the detection of ammonia in the exhaled breath sample without interference from the water vapor.

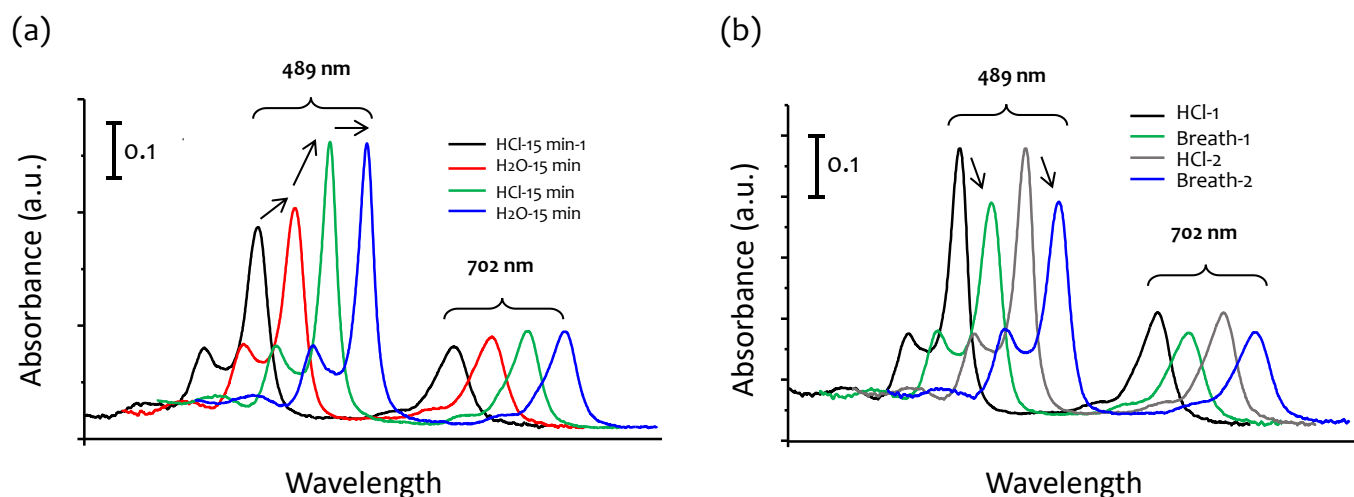


**Figure 5.** (a) UV-vis spectra of the PDDA/TSPP film: the black line represents the signal after exposure to HCl for the first 15 min, the red line represents exposure to the H<sub>2</sub>O vapor for 15 min after the first HCl exposure, the green line represents exposure to HCl for the second 15 min, and the blue line represents exposure to H<sub>2</sub>O for 15 min following HCl exposure. (b) UV-vis spectra of the PDDA/TSPP film measured after exposure to a 0.1 M HCl vapor (black and grey lines) and after exposure to breath for 10 s (green and blue lines). The spectra are shifted horizontally for illustration purposes and convenience in reading the figures.

Figure 5b shows the PDDA/TSPP film absorption spectra measured before and after exposure to two consecutive breaths. We observe that the absorption spectra measured before and after two successive breaths exhibit a relative change in the absorption spectra to the absorption spectra after the PDDA/TSPP film was exposed to ammonia. This suggests that the PDDA/TSPP film responds to the ammonia present in breath. Moreover, by using the change in absorbance (0.09 a.u.), we estimate that the concentration of exhaled ammonia is approximately 2.3 ppm (on the basis of the sensitivity of 0.04 a.u./ppm from Figure 4b).

As illustrated in Figure 2a, the absorption spectra of the PDDA/TSPP film between and/or after breath measurements can be entirely recovered by using a 0.1 M HCl solution (Figure 5b). These results support the successful application of the PDDA/TSPP film for inexpensive and reliable measurements of the ammonia gas present in human breath. At the moment of breath sampling, humidity can reach values as high as approximately 93% when breath enters the glass vial containing the PDDA/TSPP film (data not shown). Since the calibration of the PDDA/TSPP film with ammonia gas was conducted using aqueous solutions, i.e., relative humidity values near 100%, the experimental conditions are nearly identical to the breath measurements.

Regarding CO<sub>2</sub> that can potentially interfere with sensor response, its concentration in breath is extremely high; however, the developed sensor has no response to CO<sub>2</sub>, as previously confirmed [27]. Additionally, no significant sensor responses to other interfering substances present in the exhaled breath, such as acetone and some organic alcohols, have been found [28].

### 3.4. Ammonia in Urine

In addition to breath samples, the urine headspace taken from a healthy volunteer was analyzed (Figure 6a,b). Similar to both pure ammonia and breath ammonia, the

behaviors in absorption spectra were observed, particularly the decrease in absorption of the PDDA/TSPP film at 489 and 702 nm. The estimated concentration of ammonia in the urine headspace is slightly larger (2.34 ppm) than that of the breath sample (1.5 ppm) taken at the same time and from the same subject (Figure 5b). These results are in good agreement with previously published measurements using selected ion flow tube mass spectrometry (SIFT-MS) [29].

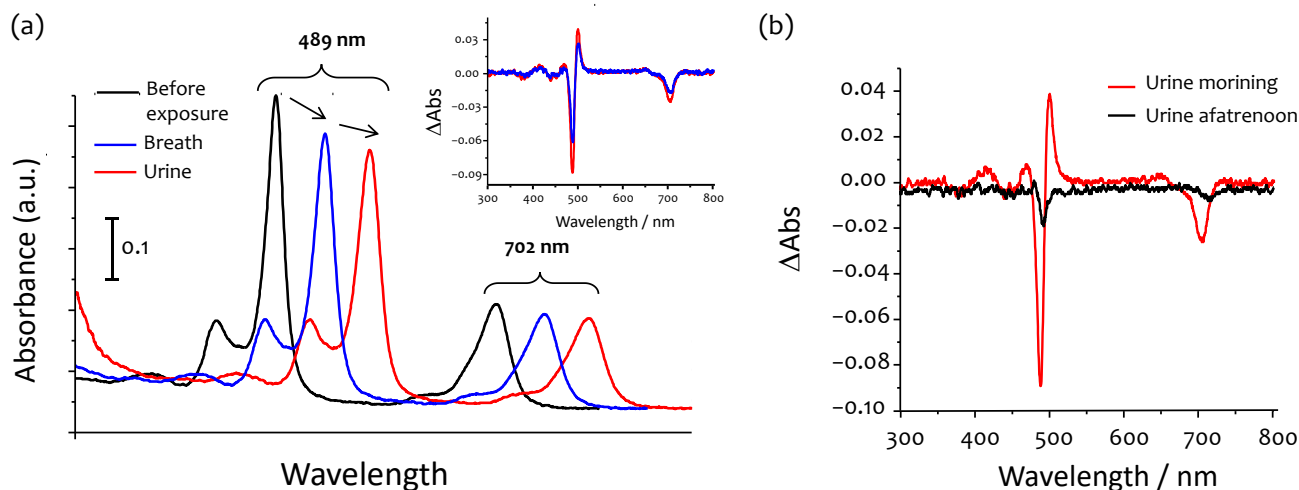


**Figure 6.** (a) UV-vis spectra of the PDDA/TSPP film measured before (after HCl vapor treatment) and after exposure to breath and urine headspace. The inset shows the corresponding difference absorption spectra. (b) Difference absorption spectra of the PDDA/TSPP film for urine samples collected in the morning and the afternoon. The spectra in Figure 6a are shifted horizontally for illustration purposes and convenience in reading the figure.

We noticed a meaningful difference in the ammonia concentration in the urine headspace depending on when the urine sample was collected, in the morning or the afternoon (Figure 6b). Variations in concentration ranged from 2.34 ppm for samples collected in the morning to 0.5 ppm for samples collected in the afternoon. In general, breath is more straightforward to analyze than urine samples that require special conditions for storage and handling. Consequently, we conducted a large-scale study by using only the breath samples.

### 3.5. Effects of Food Consumption

It is well known that ammonia concentration in a breath decreases immediately after food consumption [2]. Food habits can influence the concentration and presence of ammonia gas in the breath [29]. For example, when food with high protein content is consumed, the concentration of ammonia could increase. Moreover, breath analysis using SIFT-MS showed that levels of ammonia in the breath decreased immediately after ingesting the meal, followed by a steady increase over a 5 h period to two to three times the premeal (fasting) levels [29]. Figure 7a shows the UV-vis spectra of the PDDA/TSPP film measured before and after food consumption (breakfast). The changes in absorbance are relatively small when breath was measured immediately after food ingestion, thus suggesting that ammonia concentration is lower after ingestion than before a meal. Concentrations were 2.3 and 1.0 ppm when breath was measured before and after food consumption, respectively. These results are in agreement with the data obtained using SIFT-MS [2]. Similar behavior was observed when measurements were conducted before and after lunch (Figure 7b). Absorbance changes were smaller when the sample was measured immediately after lunch than that measured before lunch. It was also possible to obtain a stable response when two or more independent breath samples were measured (data not shown).

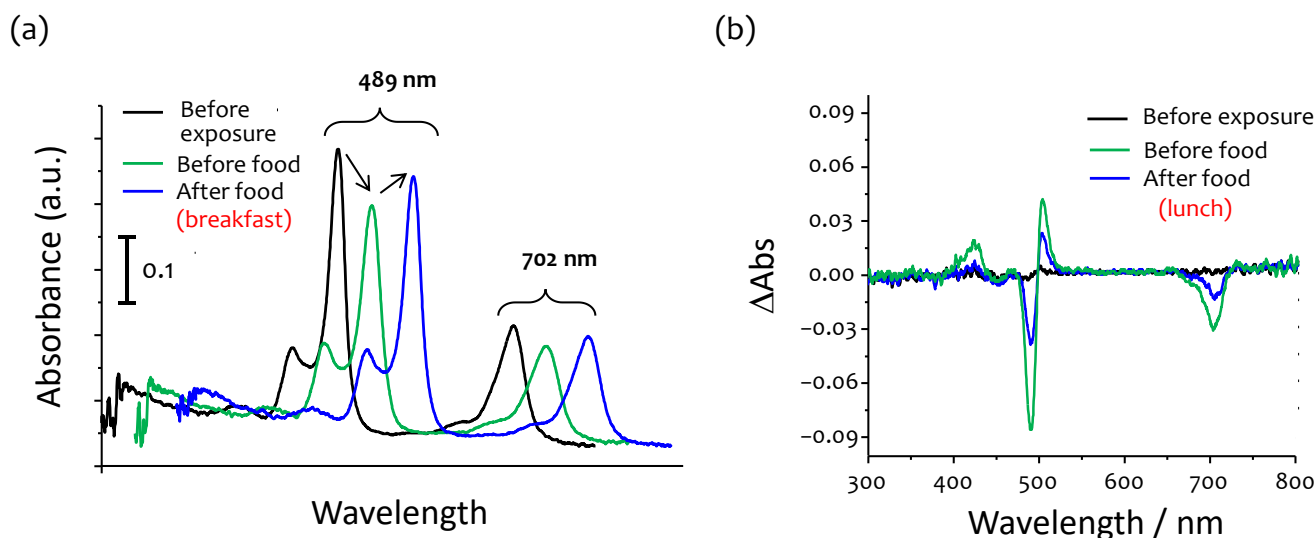


**Figure 7.** (a) UV-vis and (b) difference absorption spectra of the PDDA/TSPP film measured before (after HCl vapor treatment) and after food consumption in cases of breakfast and lunch, respectively. The spectra in Figure 7a are shifted horizontally for illustration purposes and convenience in reading the figure.

The obtained results indicate that specific food habits are important factors to be considered when designing experiments to measure ammonia concentrations in healthy and ill people. This is key to ensuring that elevated ammonia levels in breath or urine are due to disease and not different food habits. Therefore, it is necessary to investigate the detailed average fluctuation range of ammonia levels in breath or urine before and after food consumption in healthy subjects in the future.

### 3.6. Urea Test

Urea tests conducted on the basis of procedures previously described [24,25] proved the capability of the sensor to measure changes in ammonia concentration in human breath (Figure 8). A fascinating phenomenon was observed wherein there is a significant increase in the ammonia concentration in the subject's breath 5 min after urea ingestion (Figure 8a). The concentration increased from 2.3 to 10.5 ppm, followed by a return to the original value 15 min after urea ingestion (Figure 8b). The observed behavior corresponds very well with the kinetics of the interactions between urea and urease [30], i.e., ammonia reached a maximum concentration approximately 5 min after the reaction. The influence of food on the ammonia concentration in breath was also studied by conducting measurements before and after the food was consumed. When urea tests were conducted on an empty stomach, i.e., before food consumption, the ammonia concentration was much larger (10.5 ppm) than after food consumption (3.3 ppm).

### 3.7. A Large-Scale Study and Future Perspectives

The sensor was examined through a large-scale study of 41 healthy volunteers, and their breath samples were measured before and after food consumption. As mentioned above, both characteristic peaks of the respective Soret and Q bands at 489 and 702 nm have a linear correlation, as shown in Figure 9a, because they are attributed to the presence of J-aggregated TSPPs in the film. With the increase in the ammonia concentration, the absorbances of both peaks decrease, and the corresponding correlation slope leans to the lower left. This new data analysis provides more precise information on ammonia gas in the exhaled breath because other interferences that affect changes in the porphyrin aggregation are negligible. All of the 84 breath samples collected from the 41 healthy subjects, which were measured before and after food consumption, are distributed near the calibration curve, and most of them are observed below 1 ppm.

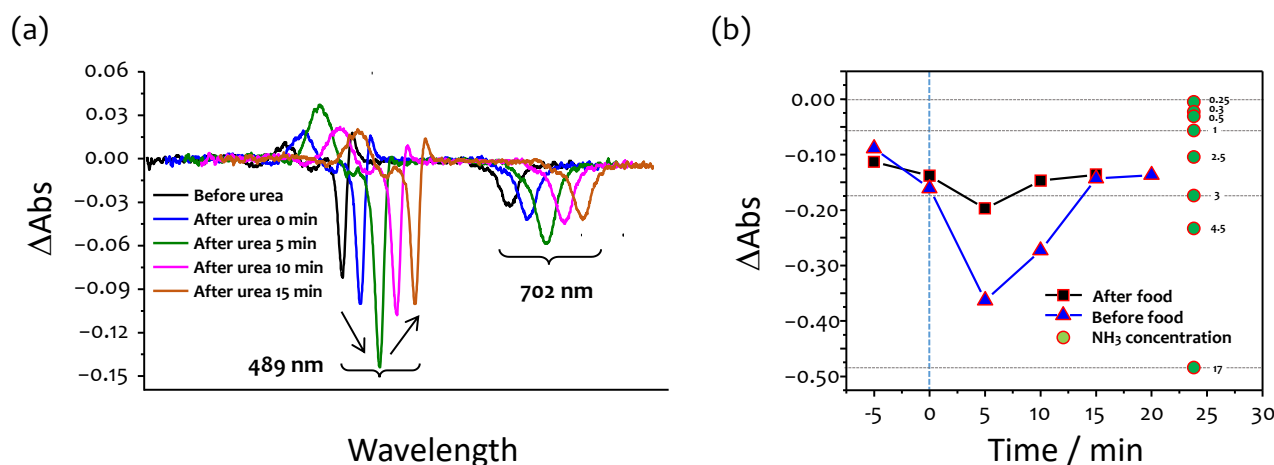


**Figure 8.** (a) Difference absorption spectra measured before and at different intervals after the consumption of 5 mL of a 1 mM aqueous urea solution. (b) Dynamic changes in absorbance measured at 489 nm after drinking the 1 mM of urea solution: the black (squares) and blue (triangles) lines represent concentrations measured after food consumption and on an empty stomach (before food consumption), respectively; green circles map the concentrations of ammonia derived from the calibration curve (Figure 4c). The spectra in Figure 8a are shifted horizontally for illustration purposes and convenience in reading the figure.

Figure 9b compares breath ammonia concentrations before and after lunch for 26 and 22 subjects, respectively (Figure S3a,b). Volunteers were asked to provide information on smoking habits, drinking habits, diet, and age. The results agree with previously published measurements using SIFT-MS techniques [2]. In particular, the ammonia concentration for all participants decreased immediately after food consumption. The ammonia concentration for a subject over 65 years of age was elevated up to approximately 1.5 ppm in the morning (before lunch). In contrast, the ammonia level was less than 0.5 ppm for most of the subjects. No correlation between smoking and drinking habits was observed. In general, for all healthy volunteers who participated in this study, the concentration of ammonia ranged between 0.3 and 1.5 ppm, with a mean value of ca. 520 ppb in the morning (before lunch) and ca. 420 ppb in the afternoon (immediately after eating).

Recently, Pandey et al. [31] reported the development of a chemoresistive ammonia sensor based on polysaccharide/gold nanocomposite. The proposed sensor is capable of operating over a wide range of concentrations (0.1 ppm to 75,000 ppm) and was used to measure ammonia in both urine and blood serum samples. Toda et al. [32] detected the concentration of exhaled ammonia by forming a film of dilute H<sub>2</sub>SO<sub>4</sub> formed on the top of two metal capillary tubes with a concentric annular arrangement. This method decreases the conductivity of the solution when ammonia passes through the tube. The sensor exhibited a linear response between the range of 200–900 ppb and was tested on one subject whose exhaled breath was sampled at a constant rate from the mask outlet. Brannelly et al. [14] proposed an electrochemical sensor to measure ammonia in the blood. The device uses a 52  $\mu$ L serum sample and an impedance-change induced by ammonia. The device is highly sensitive and has an LOD of 12  $\mu$ M ( $n = 3$ ). Results from measurements with the device ranged between 25–200  $\mu$ M with an LOD of 12  $\mu$ M ( $n = 3$ ). Unfortunately, the device has no significant issues with common electrochemical interferences in blood [15]. Recently, quartz-enhanced photoacoustic spectroscopy was used for fast and accurate ammonia measurements in exhaled breath [33]. However, this sensor requires an expansive quantum cascade laser, thus making it difficult to implement in point-of-care applications.

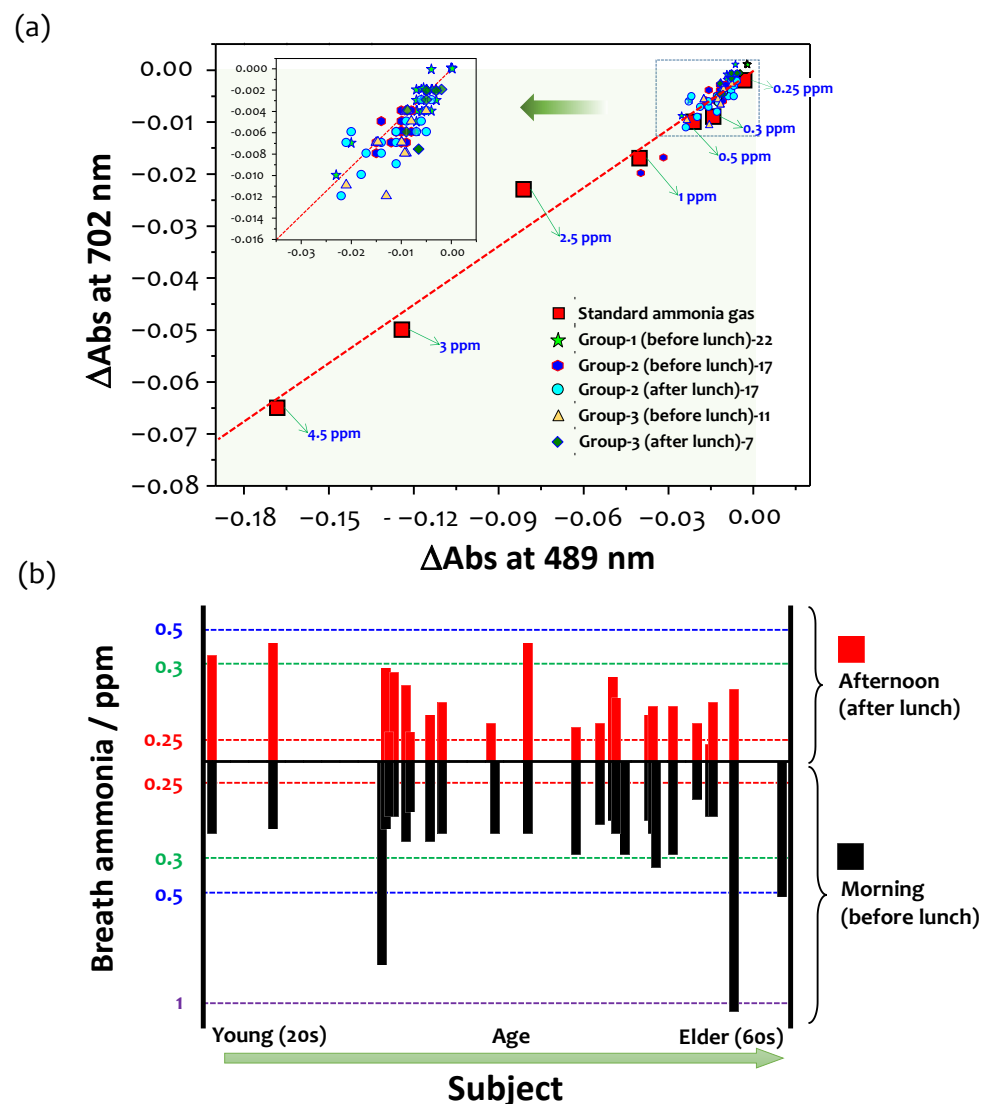


**Figure 9.** (a) A linear correlation between both characteristic peaks of the respective Soret and Q bands at 489 and 702 nm, respectively, including 84 breath samples collected from the 41 healthy subjects before and after food consumption. (b) A comparison of breath ammonia concentrations before and after food consumption for 26 and 22 healthy subjects, respectively, where the Y-axis was estimated from the sum of the absorbance changes at 489 and 702 nm.

On the other hand, optical fiber sensors can compensate for the essential drawbacks of conventional sensor devices in terms of practicality. Wolfbeis measured fluorescence by using an optical fiber probe in a pH indicator solution [34]. Since then, several approaches based on the evanescent wave [35–37], reflection [38,39], lossy mode resonance [40], and grating [40] have emerged. Sensitivity for these techniques generally ranges from tens to hundreds of ppm. Table 1 summarizes the parameters reported in the literature for ammonia optical sensors. To the best of our knowledge, the current study is the first case to test breath ammonia directly in dozens of healthy volunteers in their 20 s to 60 s. Ammonia concentrations in their exhaled breath could be estimated to be around 1 ppm, according to the literature [1,2,8].

**Table 1.** A summary of optical sensing approaches for ammonia detection.

Type of Sensor	Sensitive Element	Lower Detection Limit (LDL) or Lowest Measured Concentration (LMC)	Response Time	Reference
Evanescent wave	Universal pH indicator	10 ppm (LMC)	5 min	[35]
	Bromocresol purple/bromocresol green, dip coating sol-gel	9 ppm (LMC) 0.014 dB/ppm	8 s	[36]
	Bromocresol purple, sol-gel	145 ppm (LMC)	10 s	[37]
	Nanoassembled PDDA/TSPP	6 ppm	15 s	[20,21]
Reflection	Nanoassembled ZrO <sub>2</sub> /PSS *	1 wt% (LMC)	-	[38]
	Oxazine 170 perchlorate	200 ppm (LMC)	-	[39]
Lossy mode resonance	TMPyP **-doped TiO <sub>2</sub> nanocoating	0.1 ppm (LMC)	30 s	[40]
Grating	Nanoassembled PDDA/TSPP	0.67 ppm (LDL)	-	[41]

\* PSS: poly(sodium-4-styrenesulfonate); \*\* TMPyP: tetrakis(1-methylpyridinium-4-yl)porphyrin *p*-toluenesulfonate.

#### 4. Conclusions

To the best of our knowledge, there is no optical sensor capable of measuring ammonia in breath with the required sensitivity and selectivity for healthcare applications because of the harsh conditions in which the sensor must operate, namely, high levels of humidity, CO<sub>2</sub>, and complex sample matrices consisting of various gas compounds.

In this study, we introduced a newly developed optical ammonia sensor and successfully used it to measure ammonia in breath and urine samples collected from 41 healthy volunteers. The sensor is based on an ultrathin film of TSPP/PDDA deposited onto a quartz substrate using the LbL method. The sensor was calibrated in the lab with known concentrations of ammonia before measuring real-life samples, which showed high sensitivity with an LOD of 102 ± 12 ppb and high selectivity over water vapor toward ammonia. In general, the concentration of ammonia for the healthy volunteers who participated in this study ranged between 0.3 and 1.5 ppm, with a mean value of ca. 520 ppb in the morning (before eating) and ca. 420 ppb in the afternoon (immediately after eating). We noticed a large difference in the ammonia concentration in the urine headspace depending on the sampling time in a day. Variations in concentration ranged from 2.3 ppm for samples collected in the morning to 0.5 ppm for samples collected in the afternoon.

Previously reported procedures for the *Helicobacter pylori* (HELIC Ammonia Breath) test based on urea reaction with urease were reproduced using the proposed sensor. There is a significant increase in the ammonia concentration from 2.3 to 10.5 ppm in the subject's breath 5 min after urea ingestion, followed by a return to the original value 15 min after urea ingestion. The results obtained from the current study are in good agreement with previously reported results using SIFT-MS techniques [2]. The advantages of the proposed sensor are its compactness, simplicity, cost, and high sensitivity, and its selectivity toward ammonia. We believe that this preliminary study provides the possibility for medical applications to realize the early diagnosis of kidney, stomach, or liver disease. These diseases have surged during the recent COVID-19 pandemic and ammonia will, undoubtedly, be recognized as a more important biomarker than ever before.

**Supplementary Materials:** The following are available online at <https://www.mdpi.com/article/10.3390/chemosensors9090269/s1>, Table S1: Relationships between the concentrations of NH<sub>4</sub>OH in the solution and the corresponding gas concentrations in the headspace, Figure S1: UV-vis spectra of the PDDA/TSPP film measured after (a) exposure to ammonia vapors produced by various concentrations of ammonia solutions and (b) continuous exposures to water vapor for 15 min each after HCl vapor treatment, Figure S2: Difference absorption spectra of the three blank measurements before exposure to ammonia gas. Figure S3: Difference absorption spectra of the PDDA/TSPP film measured for the selected breath samples collected from 20 volunteers (a) before lunch and (b) after lunch.

**Author Contributions:** Conceptualization, S.-W.L.; methodology, S.K. and S.-W.L.; software, S.K.; validation, S.K.; formal analysis, S.K.; investigation, S.K. and S.-W.L.; data curation, S.K.; writing—original draft preparation, S.K.; writing—review and editing, S.-W.L.; supervision, S.-W.L.; project administration, S.-W.L.; funding acquisition, S.-W.L. All authors have read and agreed to the published version of the manuscript.

**Funding:** This work was supported by the 2nd Kitakyushu Knowledge-based Cluster Project from the Ministry of Education, Culture, Sports, Science and Technology.

**Institutional Review Board Statement:** Not applicable.

**Informed Consent Statement:** All subjects gave their informed consent for inclusion before they participated in the study.

**Data Availability Statement:** Not applicable.

**Acknowledgments:** We kindly acknowledge all participants (volunteers) for providing breath or urine samples for this study.

**Conflicts of Interest:** The authors declare no conflict of interest.

## References

1. Brannelly, N.T.; Hamilton-Shield, J.P.; Killard, A.J. The measurement of ammonia in human breath and its potential in clinical diagnostics. *Crit. Rev. Anal. Chem.* **2016**, *46*, 490–501. [[CrossRef](#)]
2. Turner, C.; Spanel, P.; Smith, D. A longitudinal study of ammonia, acetone and propanol in the exhaled breath of 30 subjects using selected ion flow tube mass spectrometry, SIFT-MS. *Physiol. Meas.* **2006**, *27*, 321–337. [[CrossRef](#)]
3. Liu, L.; Fei, T.; Guan, X.; Zhao, H.; Zhang, T. Humidity-activated ammonia sensor with excellent selectivity for exhaled breath analysis. *Sens. Actuators B Chem.* **2021**, *334*, 129625. [[CrossRef](#)]
4. Shahmoradi, A.; Hosseini, A.; Akbarinejad, A.; Alizadeh, N. Noninvasive detection of ammonia in the breath of hemodialysis patients using a highly sensitive ammonia sensor based on a polypyrrole/sulfonated graphene nanocomposite. *Anal. Chem.* **2021**, *93*, 6706–6714. [[CrossRef](#)] [[PubMed](#)]
5. Bannov, A.G.; Popov, M.V.; Brester, A.E.; Kurmashov, P.B. Recent advances in ammonia gas sensors based on carbon nanomaterials. *Micromachines* **2021**, *12*, 186. [[CrossRef](#)]
6. Barsotti, R.J. Measurement of ammonia in blood. *J. Pediatr.* **2001**, *138*, S11–S20. [[CrossRef](#)] [[PubMed](#)]
7. Metz, M.P. Ammonia, a troublesome analyte. *Clin. Biochem.* **2014**, *47*, 753. [[CrossRef](#)]
8. Španěl, P.; Smith, D. What is the real utility of breath ammonia concentration measurements in medicine and physiology? *J. Breath Res.* **2018**, *12*, 027102. [[CrossRef](#)] [[PubMed](#)]
9. Larson, T.V.; Covert, D.S.; Frank, R. A Method for continuous measurement of ammonia in respiratory airways. *J. Appl. Physiol.* **1979**, *46*, 603–607. [[CrossRef](#)] [[PubMed](#)]
10. Wakabayashi, H.; Kuwabara, Y.; Murata, H.; Kobashi, K.; Watanabe, A. Measurement of the Expiratory Ammonia Concentration and Its Clinical Significance. *Metab. Brain Dis.* **1997**, *12*, 161–169. [[CrossRef](#)] [[PubMed](#)]
11. DuBois, S.; Eng, S.; Bhattacharya, R.; Rulyak, S.; Hubbard, T.; Putnam, D.; Kearney, D.J. Breath ammonia testing for diagnosis of hepatic encephalopathy. *Dig. Dis. Sci.* **2005**, *50*, 1780–1784. [[CrossRef](#)]
12. Schmidt, F.M.; Vaittinen, O.; Metsälä, M.; Lehto, M.; Forsblom, C.; Groop, P.H.; Halonen, L. Ammonia in breath and emitted from skin. *J. Breath Res.* **2013**, *7*, 017109. [[CrossRef](#)] [[PubMed](#)]
13. Germanese, D.; Colantonio, S.; D’Acunto, M.; Romagnoli, V.; Salvati, A.; Brunetto, M. An E-Nose for the Monitoring of Severe Liver Impairment: A Preliminary Study. *Sensors* **2019**, *19*, 3656. [[CrossRef](#)]
14. Brannelly, N.T.; Killard, A.J. An electrochemical sensor device for measuring blood ammonia at the point of care. *Talanta* **2017**, *167*, 296–301. [[CrossRef](#)]
15. Timmer, B.; Olthuis, W.; van den Berg, A. Ammonia sensors and their applications—A review. *Sens. Actuators B Chem.* **2005**, *107*, 666–677. [[CrossRef](#)]
16. Wang, T.; Pysanen, A.; Dryahina, K.; Španěl, P.; Smith, D. Analysis of breath, exhaled via the mouth and nose, and the air in the oral cavity. *J. Breath Res.* **2008**, *2*, 037013. [[CrossRef](#)]
17. Hibbard, T.; Killard, A.J. Breath ammonia analysis: Clinical application and measurement. *Crit. Rev. Anal. Chem.* **2011**, *41*, 21–35. [[CrossRef](#)]
18. Korposh, S.; Selyanchyn, R.; Yasukochi, W.; Lee, S.-W.; James, S.; Tatam, R. Optical fibre long period grating with a nanoporous coating formed from silica nanoparticles for ammonia sensing in water. *Mater. Chem. Phys.* **2012**, *133*, 784–792. [[CrossRef](#)]
19. Wang, T.; Korposh, S.; James, S.; Tatam, R.; Lee, S.-W. Optical fiber long period grating sensor with a polyelectrolyte alternate thin film for gas sensing of amine odors. *Sens. Actuators B Chem.* **2013**, *185*, 117–124. [[CrossRef](#)]
20. Korposh, S.; Kodaira, S.; Selyanchyn, R.; Ledezma, F.H.; James, S.W.; Lee, S.-W. Porphyrin-nanoassembled fiber-optic gas sensor fabrication: Optimization of parameters for sensitive ammonia gas detection. *Opt. Laser Technol.* **2018**, *101*, 1–10. [[CrossRef](#)]

21. Korposh, S.O.; Takahara, N.; Ramsden, J.J.; Lee, S.-W.; Kunitake, T. Nano-assembled thin film gas sensors. I. Ammonia detection by a porphyrin-based multilayer film. *J. Biol. Phys. Chem.* **2006**, *6*, 125–133. [[CrossRef](#)]
22. Davies, S.; Spanel, P.; Smith, D. Quantitative analysis of ammonia on the breath of patients in end-stage renal failure. *Kidney Int.* **1997**, *52*, 223–228. [[CrossRef](#)] [[PubMed](#)]
23. Mochalski, P.; King, J.; Haas, M.; Unterkofler, K.; Amann, A.; Mayer, G. Blood and breath profiles of volatile organic compounds in patients with end-stage renal disease. *BMC Nephrol.* **2014**, *15*, 43. [[CrossRef](#)] [[PubMed](#)]
24. Kusters, J.G.; Vliet, A.H.M.; Kuipers, E.J. Pathogenesis of helicobacter pylori infection. *Clin. Microbiol. Rev.* **2006**, *19*, 449–490. [[CrossRef](#)] [[PubMed](#)]
25. Kornienko, E.A.; Dmitrienko, M.A. A rapid urease test and helicobacter ammonia breath test for *H. pylori* detection. In *Handbook for Specialists*; Saint-Petersburg State Pediatric Medicine Academy: Saint-Petersburg, Russia, 2010.
26. Desimoni, E.; Brunetti, B. About Estimating the Limit of Detection by the Signal to Noise Approach. *Pharm. Anal. Acta* **2015**, *6*, 355.
27. Liu, L.; Morgan, S.P.; Correia, R.; Lee, S.-W.; Korposh, S. Multi-Parameter Optical Fiber Sensing of Gaseous Ammonia and Carbon Dioxide. *J. Light. Technol.* **2020**, *38*, 2037–2045. [[CrossRef](#)]
28. Ahmed, S.; Park, Y.; Okuda, H.; Ono, S.; Korposh, S.; Lee, S.-W. Fabrication of Humidity-Resistant Optical Fiber Sensor for Ammonia Sensing using Diazo Resin-Photocrosslinked Films with a Porphyrin-Polystyrene Binary Mixture. *Sensors* **2021**, *21*, 6176. [[CrossRef](#)]
29. Diskin, A.M.; Spanel, P.; Smith, D. Increase of acetone and ammonia in urine headspace and breath during ovulation quantified using selected ion flow tube mass spectrometry. *Physiol. Meas.* **2003**, *24*, 191–199. [[CrossRef](#)] [[PubMed](#)]
30. Hu, G.; Pojman, J.A.; Scott, S.K.; Wrobel, M.M.; Taylor, A.F. Base-catalyzed feedback in the urea-urease reaction. *J. Phys. Chem. B* **2010**, *114*, 14059–14063. [[CrossRef](#)]
31. Pandey, S.; Nanda, K.K. Au nanocomposite based chemiresistive ammonia sensor for health monitoring. *ACS Sens.* **2016**, *1*, 55–62. [[CrossRef](#)]
32. Toda, K.; Li, J.; Dasgupta, P.K. Measurement of ammonia in human breath with a liquid-film conductivity sensor. *Anal. Chem.* **2006**, *78*, 7284–7291. [[CrossRef](#)]
33. Solga, S.F.; Mudalel, M.L.; Spacek, L.A.; Risby, T.H. Fast and accurate exhaled breath ammonia measurement. *J. Vis. Exp.* **2014**, *88*, 51658. [[CrossRef](#)]
34. Wolfbeis, O.S.; Posch, H.E. Fibre-optic fluorescing sensor for ammonia. *Anal. Chim. Acta* **1986**, *185*, 321–327. [[CrossRef](#)]
35. Rodríguez, A.J.; Zamarreño, C.R.; Matías, I.R.; Arregui, F.J.; Domínguez Cruz, R.F.; May-Arrijoja, D.A. A fiber optic ammonia sensor using a universal pH indicator. *Sensors* **2014**, *143*, 4060–4073. [[CrossRef](#)]
36. Yagi, T.; Kuboki, N.; Suzuki, Y.; Uchino, N.; Nakamura, K.; Yoshida, K. Fiber-optic ammonia sensors utilizing rectangular-cladding eccentric-core fiber. *Opt. Rev.* **1997**, *4*, 596–600. [[CrossRef](#)]
37. Cao, W.; Duan, Y. Optical fiber-based evanescent ammonia sensor. *Sens. Actuators B Chem.* **2005**, *110*, 252–259. [[CrossRef](#)]
38. Galbarra, D.; Arregui, F.J.; Matias, I.R.; Claus, R.O. Ammonia optical fiber sensor based on self-assembled zirconia thin films. *Smart Mater. Struct.* **2005**, *14*, 739–744. [[CrossRef](#)]
39. Chu, C.-S.; Chen, Y.-F. Development of ratiometric optical fiber sensor for ammonia gas detection. In *25th Optical Fiber Sensors Conference (OFS), Proceedings of the SPIE 10323, Jeju, Korea, 23 April 2017*; International Society for Optical Engineering: Washington, DC, USA, 2017; Volume 10323, p. 103231P. [[CrossRef](#)]
40. Tiwari, D.; Mullaney, K.; Korposh, S.; James, S.W.; Lee, S.-W.; Tatam, R.P. An ammonia sensor based on Lossy Mode Resonances on a tapered optical fibre coated with porphyrin-incorporated titanium dioxide. *Sens. Actuators B Chem.* **2017**, *242*, 645–652. [[CrossRef](#)]
41. Wang, T.; Yasukochi, W.; Korposh, S.; James, S.W.; Tatam, R.P.; Lee, S.-W. A long period grating optical fiber sensor with nano-assembled porphyrin layers for detecting ammonia gas. *Sens. Actuators B Chem.* **2016**, *228*, 573–580. [[CrossRef](#)]